

Appendix–Supplementary information for:

Ribonucleic Acid as an Intrinsically Synergistic Bio-Derived Flame Retardant

Sang Yun Jeong[¶], Jong Seok Lim[¶], Abdullah Malik, Jae Chul Ro, Hui Hun Cho*, Jun Hyuk Heo*, Jung Heon Lee*

[¶] These authors contributed equally to this work

S. Y. Jeong, J. S. Lim, A. Malik, J.C. Ro, H. H. Cho, J. H. Heo, J. H. Lee

School of Advanced Materials Science and Engineering, Sungkyunkwan University (SKKU),
Suwon 16419, South Korea

H. H. Cho, J. H. Heo, J. H. Lee

Research Center for Advanced Materials Technology, SKKU, Suwon 16419, South Korea

J. H. Lee

Biomedical Institute for Convergence at SKKU, SKKU, Suwon 16419, South Korea

J. H. Lee

SKKU Advanced Institute of Nanotechnology, SKKU, Suwon 16419, South Korea

E-mail: studisthun@skku.edu (H. H. Cho), saegusa@skku.edu (J. H. Heo), jhlee7@skku.edu
(J. H. Lee)

Supplementary Contents

Fig. S1. Molecular structure comparison of RNA and DNA highlighting the key chemical differences relevant to flame-retardant behavior.

Fig. S2. Comparison of the chemical state between RNA and DNA via FTIR.

Fig. S3. Thermal behaviors of Uracil and Thymine. (a) TGA, (b) DSC, and (c) DTA.

Fig. S4. Optimization of RNA concentration through TGA analysis.

Fig. S5. Comparative thermal analyses of RNA-PUF and DNA-PUF. (a) TGA, (b) DSC, and (c) DTA.

Fig. S6. Comparison of thermal degradation behavior between RNA-PUF and DNA-PUF through DTG curves.

Fig. S7. UL-94 HBF test for DNA-PUF.

Fig. S8. UL-94 HBF test for RNA-PUF after aging and water immersion.

Fig. S9. UL-94 HBF test for DNA-PUF after aging and water immersion.

Fig. S10. Photographs of RNA-PUF before and after conduction of LOI test.

Fig. S11. Cone calorimetry analysis of DNA-PUF. (a) Heat-release rate (HRR), (b) Total heat release (THR), and (c) Total smoke release (TSR) curves of bare PUF and DNA-PUF measured under an external heat flux of 35 kW/m². (d) Top-view and side-view photographs of DNA-PUF before and after cone calorimetry testing.

Fig. S12. EDS analysis results of bare PUF and RNA-PUF (B); (B) means before combustion.

Fig. S13. Tensile stress-strain curves of bare PUF, RNA-PUF, and DNA-PUF, along with the photographs of RNA-PUF during the tensile test.

Fig. S14. Investigation of recovery behavior of bare PUF, RNA-PUF, and DNA-PUF under a compression load of 3000 kPa.

Fig. S15. Comparative FTIR analysis among bare PUF, RNA, and RNA-PUF.

Fig. S16. XPS narrow-range spectra for bare PUF and RNA-PUF.

Fig. S17. STA-MS spectra of RNA thermal decomposition.

Table S1. UL94 HBF and LOI test results for RNA-PUF and DNA-PUF after aging and immersion.

Table S2. Comparison of flame retardancy evaluation of FR applied PUFs.

Video S1. Burning test on DNA and RNA pellets.

Video S2. HBF test on bare PUF and RNA-PUF.

Video S3. UL94 HBF test of DNA-PUF.

Video S4. UL-94 HBF test of RNA-PUF after aging and immersion.

Video S5. UL-94 HBF test of DNA-PUF after aging and immersion.

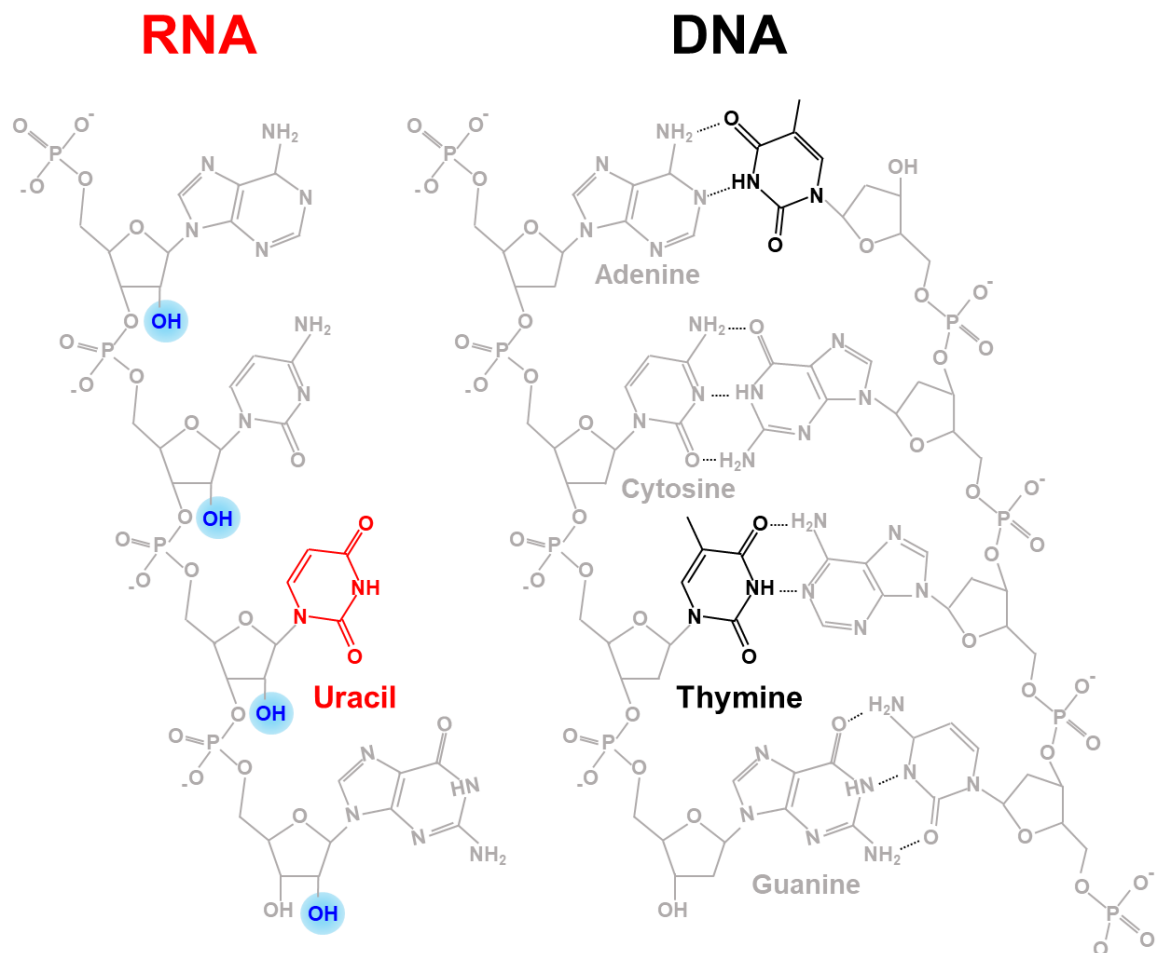


Fig S1. Molecular structure comparison of RNA and DNA highlighting the key chemical differences relevant to flame-retardant behavior.

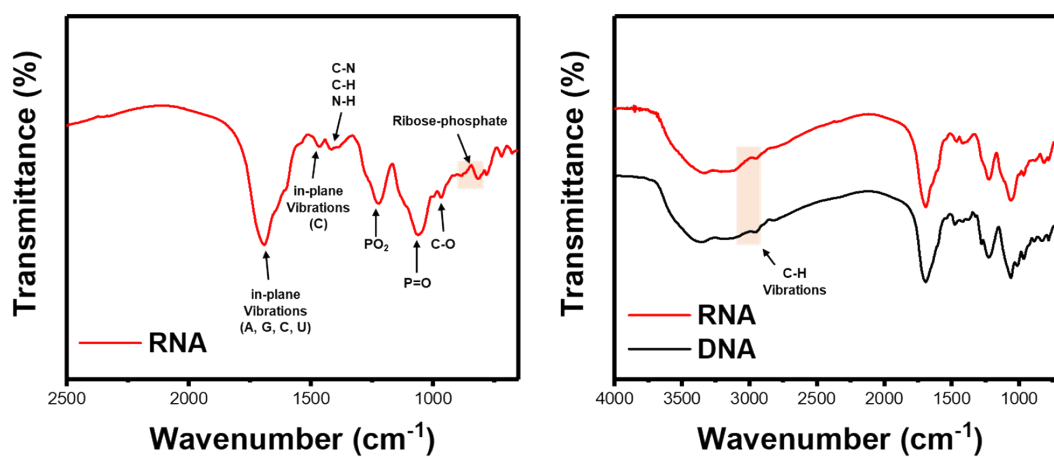


Fig. S2. Comparison of the chemical state between RNA and DNA via FTIR.

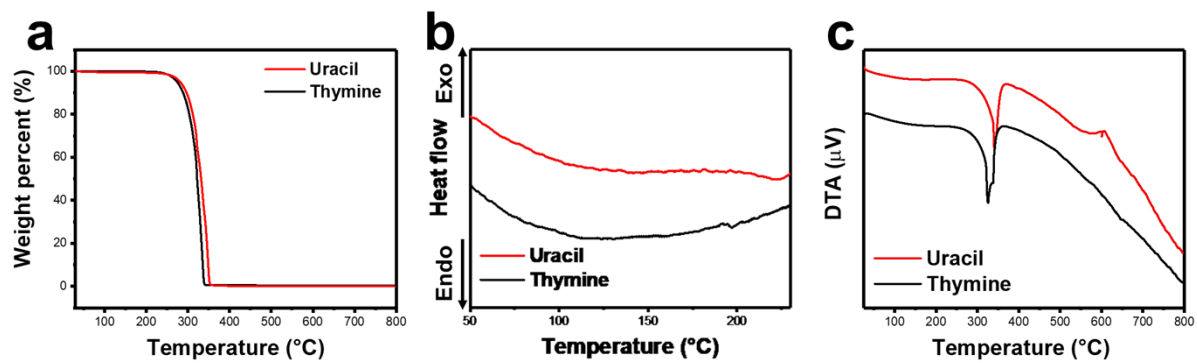


Fig. S3. Thermal behaviors of Uracil and Thymine. (a) TGA, (b) DSC, and (c) DTA.

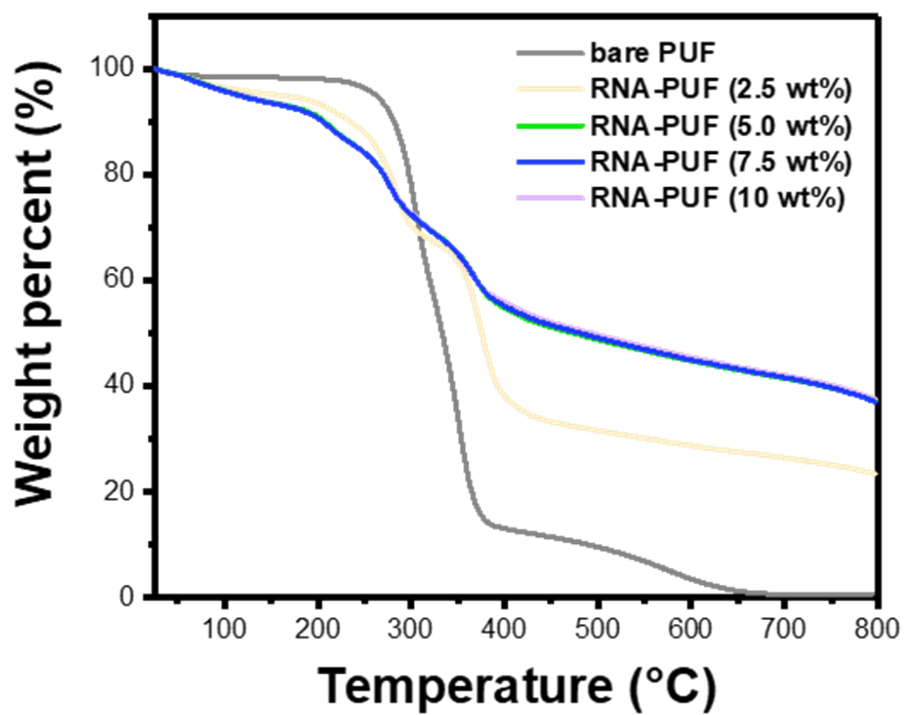


Fig. S4. Optimization of RNA concentration through TGA analysis.

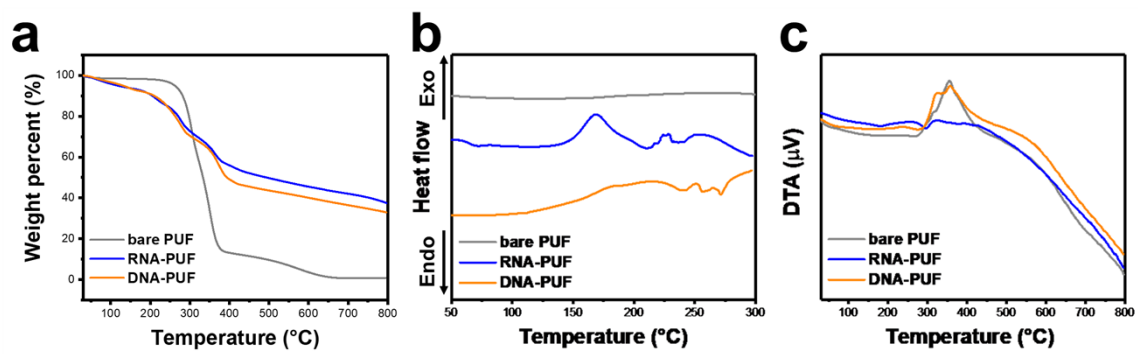


Fig. S5. Comparative thermal analyses of RNA-PUF and DNA-PUF. (a) TGA, (b) DSC, and (c) DTA.

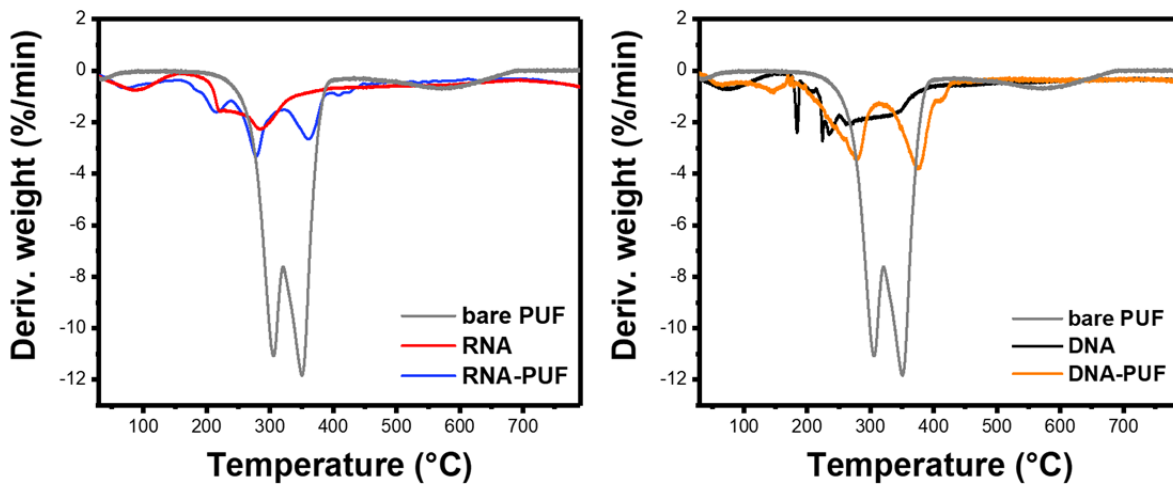


Fig. S6. Comparison of thermal degradation behavior between RNA-PUF and DNA-PUF through DTG curves.

DNA-PUF

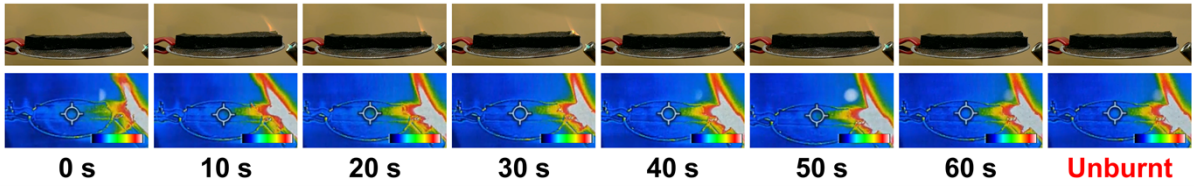
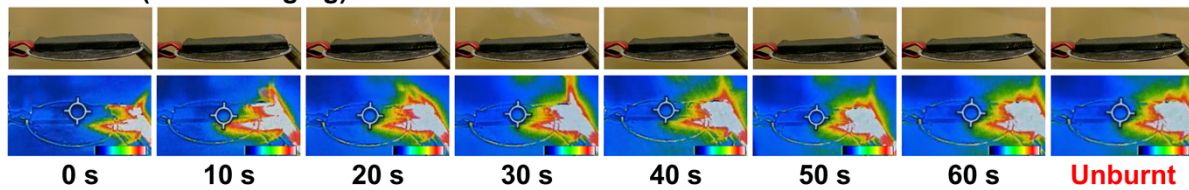
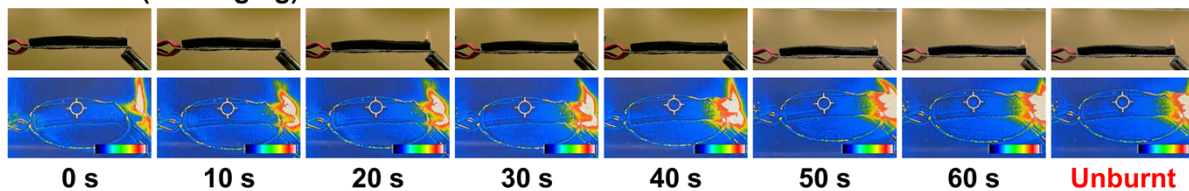


Fig. S7. UL-94 HBF test for DNA-PUF.

RNA-PUF (Ambient-aging)



RNA-PUF (Heat-aging)



RNA-PUF (Immersion)

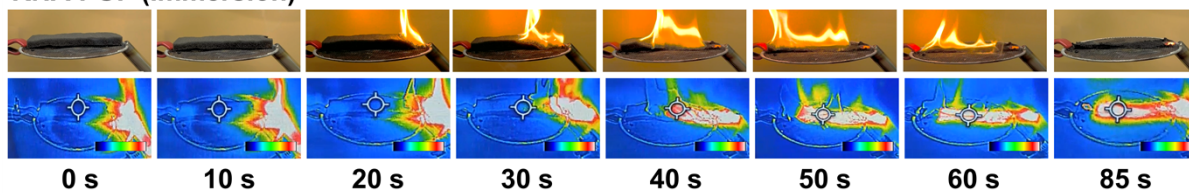
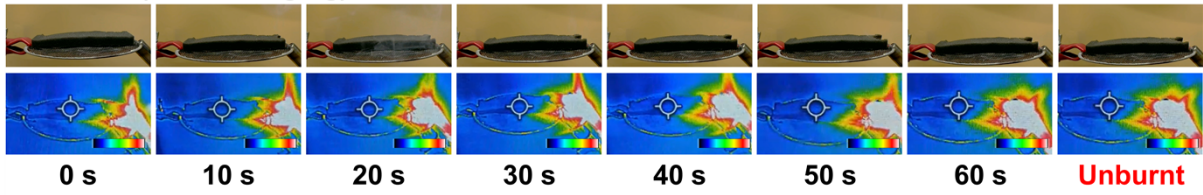
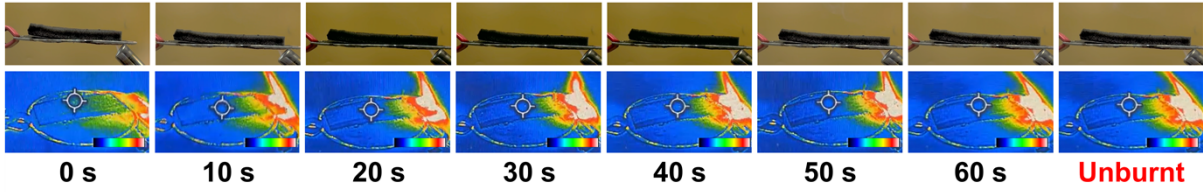


Fig. S8. UL-94 HBF test for RNA-PUF after aging and water immersion.

DNA-PUF (Ambient-aging)



DNA-PUF (Heat-aging)



DNA-PUF (Immersion)

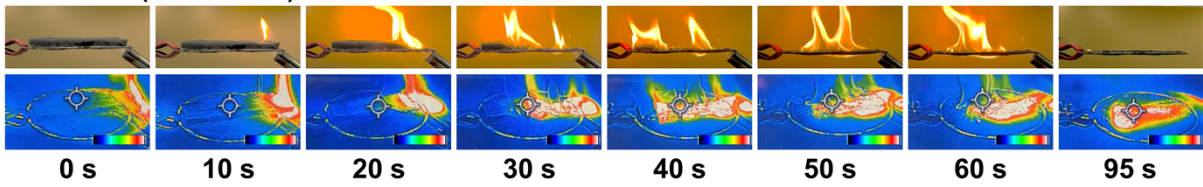


Fig. S9. UL-94 HBF test for DNA-PUF after aging and water immersion.

Before



After

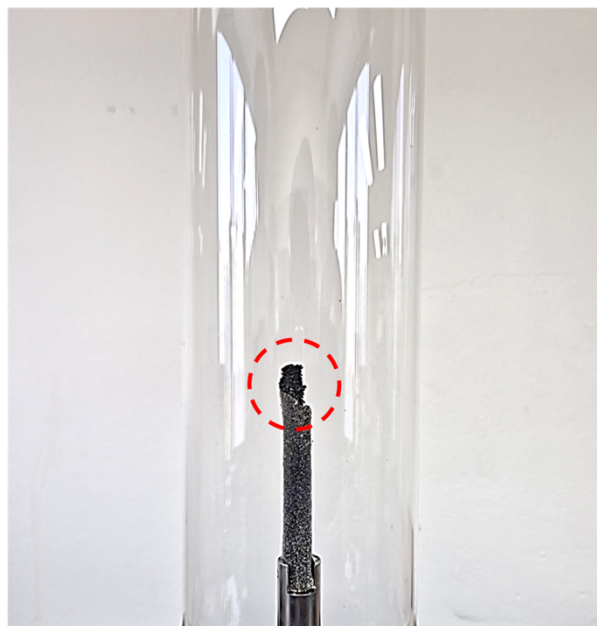


Fig. S10. Photographs of RNA-PUF before and after conduction of LOI test.

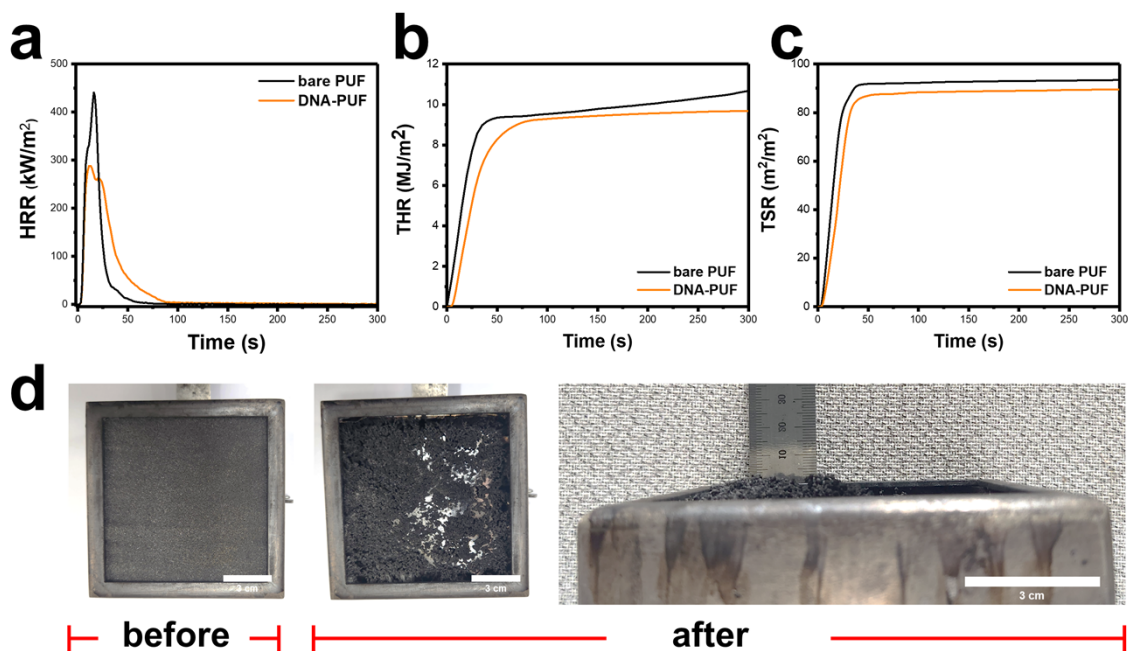


Fig. S11. Cone calorimetry analysis of DNA-PUF. (a) Heat-release rate (HRR), (b) Total heat release (THR), and (c) Total smoke release (TSR) curves of bare PUF and DNA-PUF measured under an external heat flux of 35 kW/m². (d) Top-view and side-view photographs of DNA-PUF before and after cone calorimetry testing.

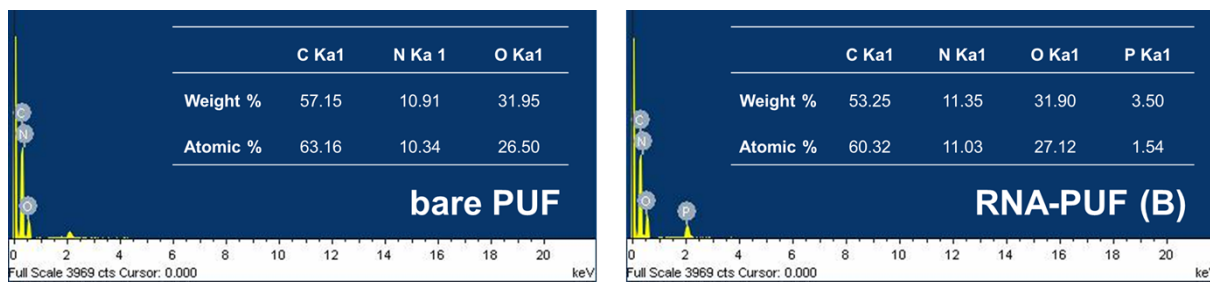


Fig. S12. EDS analysis results of bare PUF and RNA-PUF (B); (B) means before combustion.

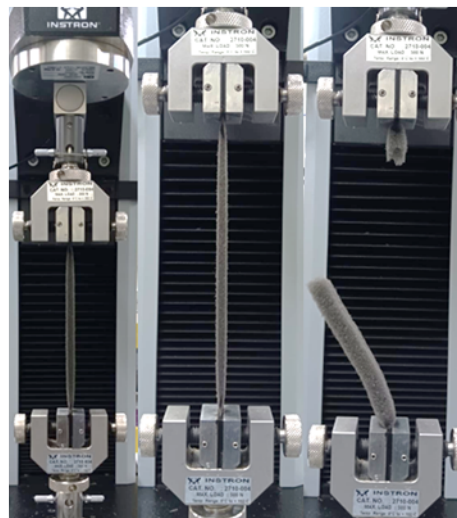
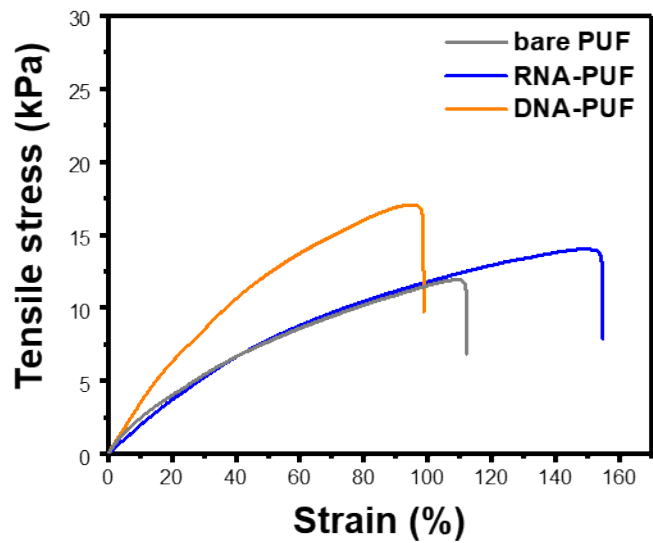


Fig. S13. Tensile stress-strain curves of bare PUF, RNA-PUF, and DNA-PUF, along with the photographs of RNA-PUF during the tensile test.

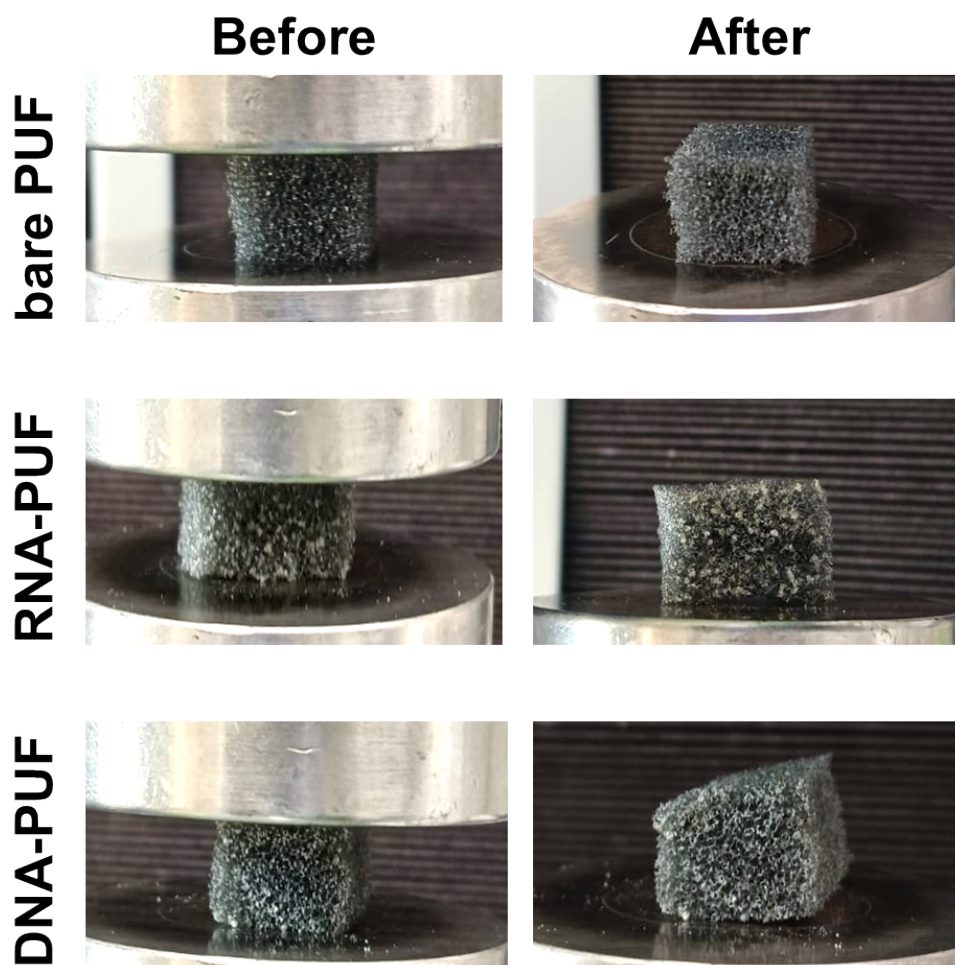


Fig. S14. Investigation of recovery behavior of bare PUF, RNA-PUF, and DNA-PUF under a compression load of 3000 kPa.

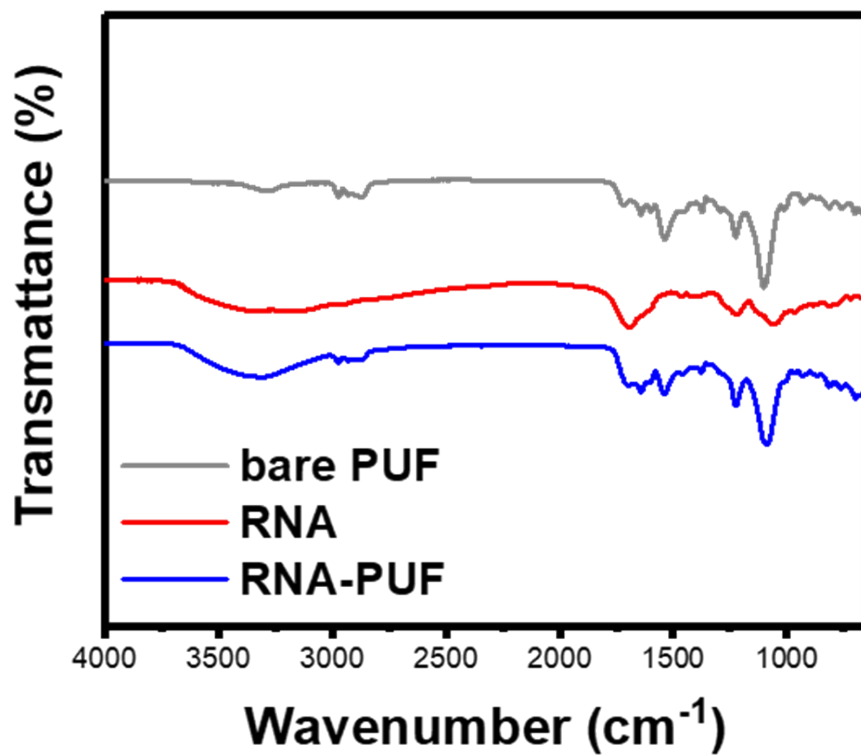


Fig. S15. Comparative FTIR analysis among bare PUF, RNA, and RNA-PUF.

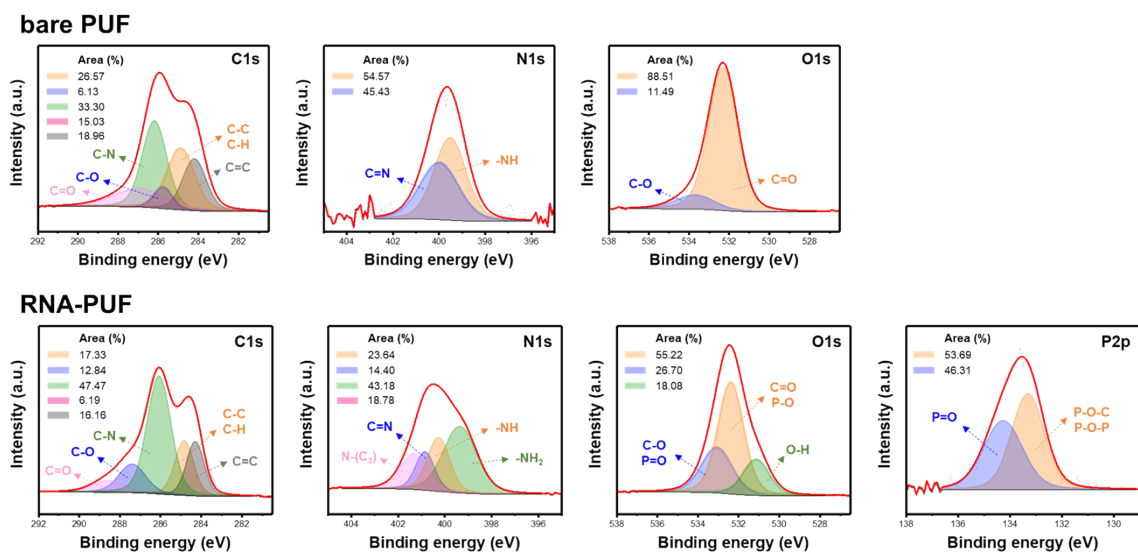


Fig. S16. XPS narrow-range spectra for bare PUF and RNA-PUF.

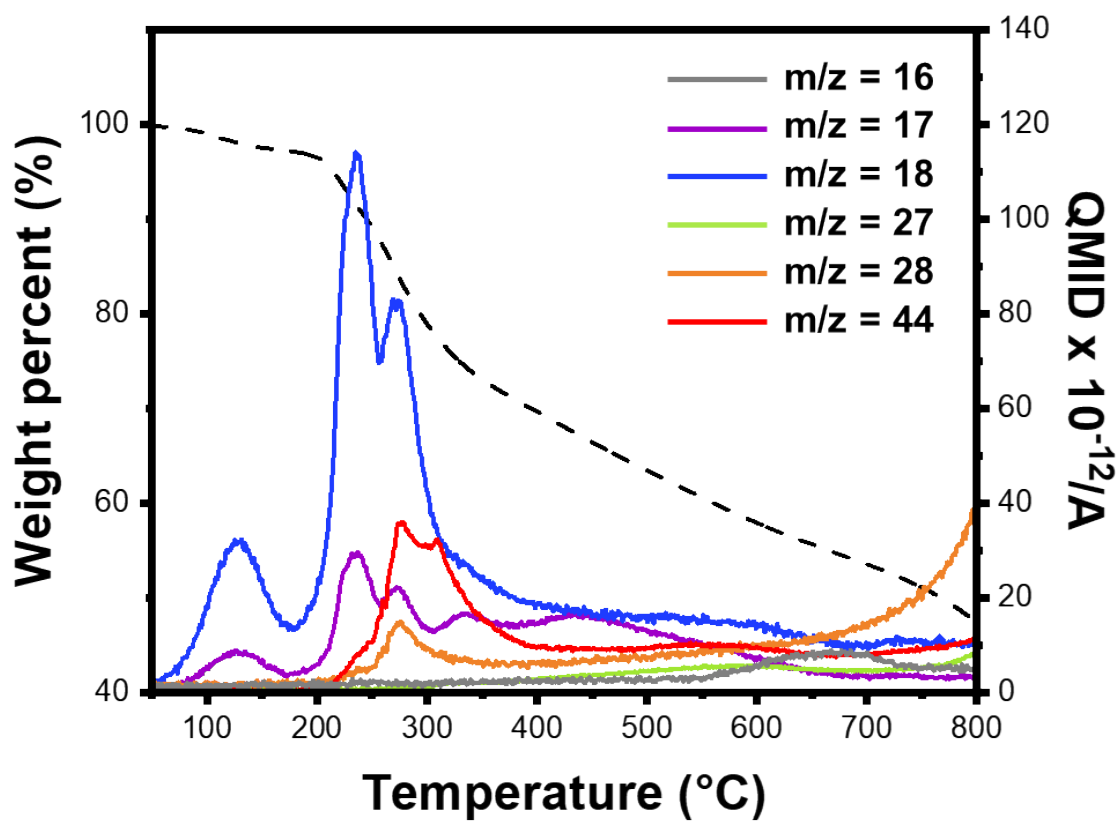


Fig. S17. STA-MS spectra of RNA thermal decomposition.

Table S1. UL94 HBF and LOI test results for RNA-PUF and DNA-PUF after aging and immersion.

Materials	Aging method	UL94 HBF test	LOI (%)
RNA-PUF	Non-treated	HF-1	29.3 ± 0.5
	Ambient	HF-1	29.2 ± 0.4
	Heat	HF-1	26.6 ± 0.8
	Immersion	NR	18.8 ± 0.1
DNA-PUF	Non-treated	HF-1	28.0 ± 0.4
	Ambient	HF-1	27.8 ± 0.5
	Heat	HF-1	24.3 ± 0.7
	Immersion	NR	17.9 ± 0.1

Materials	Applied concentration (wt%)	LOI (%)	p-HRR reduction rate (%)	Ref
RNA	5.0	29.3	49.4	This work
PFAPP/PL	30	24.5	48.1	1
ATP	20	28.0	48.0	2
MADP-DOPO	15	27.0	32.9	3
PEPS	25	27.0	30.6	4
BDMPP	20	23.0	13.5	5
CMA	30	24.1	10.8	6
DOPO-BA	20	28.1	8.5	7

Table S2. Comparison of flame retardancy evaluation of FR applied PUFs.

References

- 1 W. Xing, H. Yuan, P. zhang, H. Yang, L. Song and Y. Hu, *J. Polym. Res.*, 2013, **20**, 234.
- 2 S. H. Jeong, J. H. Heo, J. W. Lee, M. J. Kim, C. H. Park and J. H. Lee, *Acs Appl Mater Inter*, 2021, **13**, 22935–22945.
- 3 Y. Yuan, C. Ma, Y. Shi, L. Song, Y. Hu and W. Hu, *Mater. Chem. Phys.*, 2018, **211**, 42–53.
- 4 D. Wu, P. Zhao and Y. Liu, *Polym. Eng. Sci.*, 2013, **53**, 2478–2485.
- 5 F. Zhou, T. Zhang, B. Zou, W. Hu, B. Wang, J. Zhan, C. Ma and Y. Hu, *Polym. Degrad. Stab.*, 2020, **171**, 109029.
- 6 M.-J. Chen, Z.-B. Shao, X.-L. Wang, L. Chen and Y.-Z. Wang, *Ind. Eng. Chem. Res.*, 2012, **51**, 9769–9776.
- 7 M. Zhang, Z. Luo, J. Zhang, S. Chen and Y. Zhou, *Polym. Degrad. Stab.*, 2015, **120**, 427–434.